

Adaptive phase steps for diffractive phase elements using two-photon polymerization

E. I. SCARLAT^{a,*}, M. MIHAILESCU^a, N. MIHALE^b, I. A. PAUN^{a,c}, B. S. CALIN^c, C. R. LUCULESCU^c, D. TRANCĂ^a

^aApplied Sciences, Physics Dept., University Politehnica Bucharest, Romania

^bComputer Sciences, University Politehnica Bucharest, Romania

^cCETAL Group, National Institute for Laser, Plasma, and Radiation Physics, Bucharest-Magurele, Romania

Direct laser writing technique by two-photon polymerization (DLW-2PP) allows to optimize the manufacturing of diffractive phase elements (DPE) using unequal phase steps. Optimization addresses the designing stage, being adapted to the specific characteristics of the DPE. The algorithm is implemented in Python language and contains an extension consisting in two iterative loops: a local one in the phase space, and a global loop in the object space. The method is tested in the cases of relevant DPEs. The results confirm the advantage of phase mapping with unequal steps compared to equal steps.

(Received October 12, 2018; accepted April 8, 2019)

Keywords: Unequal phase steps, Local iterative loop, Holographic phase map, Python software, Two-photon photolithography

1. Introduction

Various techniques are used to cut the costs by reducing the working time and the volumes of processed materials during fabrication processes of diffractive devices [1]: diffractive elements in the case of diffraction gratings [2], diffractive lenses [3], or holograms encoding optical vortices [4] designed to produce desired field distributions for communication issues [5], optical trapping [6], or absorptive structures for solar cells [7]. Getting the desired field distribution with diffractive maps is hindered by at least two practical limitations: i/ retaining for reconstruction either only the phase or the amplitude information, and ii/ approximation with a limited number of levels of the phase shifts (or of the gray levels), often only two in the case of mask technology.

Since DLW-2PP technology is more versatile, the paper presents a method to improve DPE manufacturing in the designing stage using the approximation with unequal phase steps, here in four steps. The improvement consists in an additional loop that can further minimize the distance between the simulated multi-level phase map and its four level approximated version. The result is depending on the depths of phase steps as well as on their distribution onto the polymer surface such that the approximation with unequal phase steps is adapted to the particular DPE subjected to fabrication.

After the introductory section, Sec. 2 is briefly explaining the method, in Sec. 3 are discussed the results, and in Sec. 4 are presented the concluding remarks.

2. Method

2.1. The problem

The designing of large categories of DPEs follows a spatial light modulator (SLM) assisted, iterative processes of the type illustrated in a simplified version in Fig.1, where $O_{\delta}(x,y)$ is the optical intensity in the object plane (x,y) which optimally reproduces the desired object $O(x,y)$ with a quite large number of approximating phase levels (in most cases 256 equally spaced levels according to SLM resolution). Depending on the particular configuration of the desired field distribution, the optimization loop uses various iterated algorithms to extract the appropriate phase distribution $\Phi_{\delta}(u,v)$ that minimize a measure of distance type between $O(x,y)$ and $O_{\delta}(x,y)$ like the versatile Gerchberg-Saxton algorithm [8, 9], or more sophisticated approaches when the distribution along z -axis is required as input data [10]. Here we assume intensity distribution is localized in the diffraction plane such that the problem is two-dimensional. For a $M \times N$ object matrix the optimization accounts for minimization of the root-mean-square distance (RMSD) [11]:

$$RMSD_{object} = \sqrt{\frac{1}{MN} \sum_{x,y} |O(x,y) - O_{\delta}(x,y)|^2} \rightsquigarrow \min. \quad (1)$$

Hereafter „min” is in the sense of the lowest threshold value when the software algorithms stop and deliver the output data sets, not in the sense of a mathematical local minimum.

Whatever the algorithm, the DPEs fabrication techniques do not support but much smaller numbers of approximating phase steps $\Phi_{\Delta}(u,v)$ compared to the multi-levelled SLM optimum, i.e. $\Phi_{\Delta}(u,v) \approx \Phi_{\delta}(u,v)$, thus distorting once more the reconstructed beam from the desired pattern $O_{\Delta}(x,y) \approx O_{\delta}(x,y)$.

Fortunately, for the same number of approximating levels the DLW-2PP technology allows for better

approximations by dividing the phase range $[0,2\pi)$ in unequal steps instead of the classical uniform partition. Similarly to Eq. (1) the RDMS between the $I \times J$ matrices $\Phi_{\Delta}(u,v)$ and $\Phi_{\delta}(u,v)$ is:

$$RMSDphase = \sqrt{\frac{1}{IJ} \sum_{u,v} |\Phi_{\Delta}(u,v) - \Phi_{\delta}(u,v)|^2} \quad (2)$$

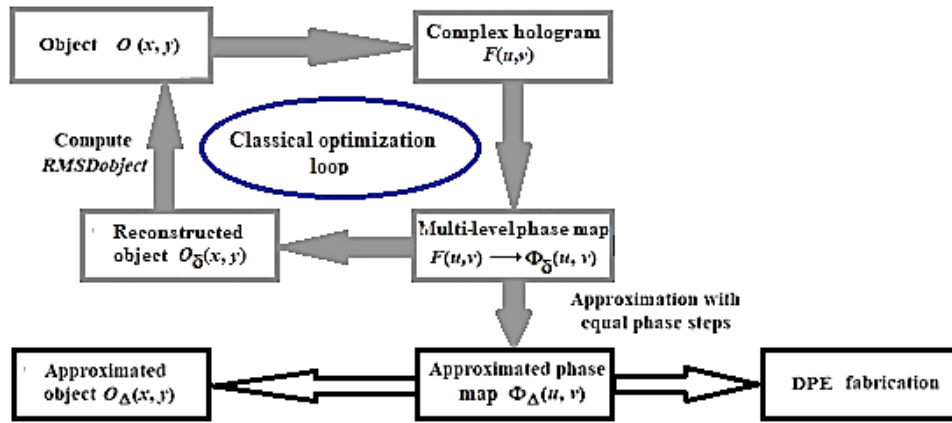


Fig.1. Classical optimization loop based on RMSDobject criterion

2.2. Unequal vs. equal steps approximation

Considering the algorithm is running with 256 levels in the phase space (consistent with the accuracy of the SLM used in our experimental simulations), for any histogram $H(\Phi_{\delta})$ of a particular phase map $\Phi_{\delta}(u,v)$, a four levels, equal steps approximation means to divide the numeric phase

range $n \in [0, 255]$ in four equally stepped levels $\{0, 64, 128, 192\}$. Level 1 is 0 if $n < 64$, level 2 is 64 if $64 \leq n < 128$, level 3 is 128 if $128 \leq n < 192$, and level 4 is 192 if $192 \leq n < 255$. The result is a four level histogram $H(\Phi_{\Delta,E})$ of an also four steps approximating phase map $\Phi_{\Delta,E}(u,v)$, as shown in Fig. 2.

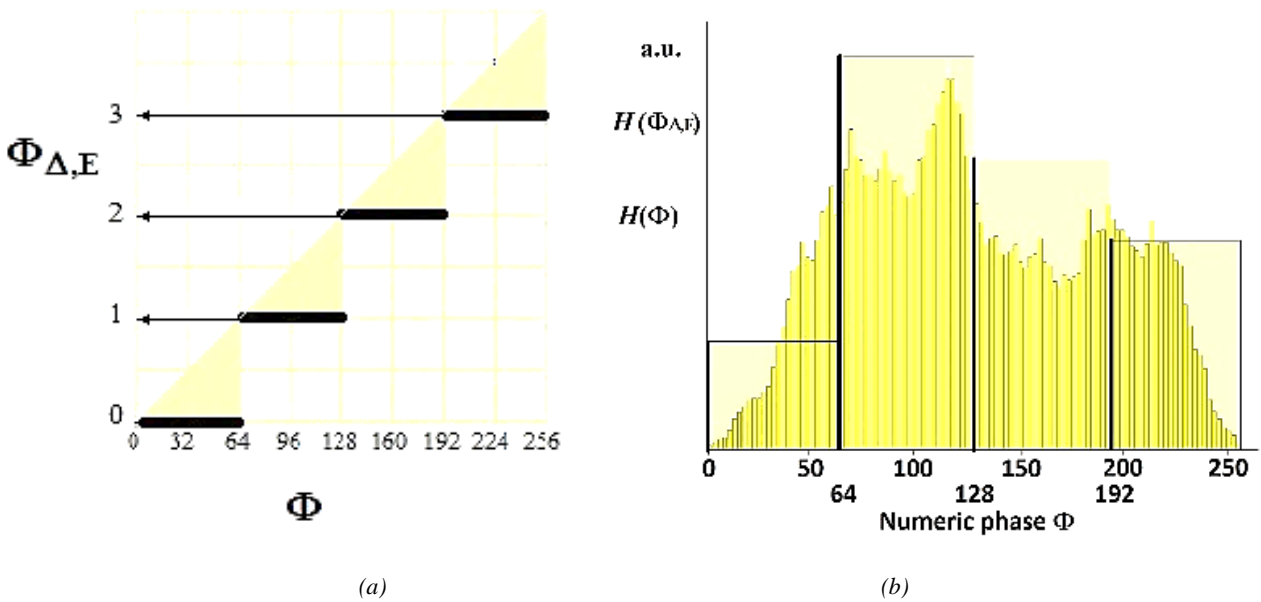


Fig. 2. (a) Approximation with equal steps: the principle, and (b) example of application on an arbitrary histogram (the histograms shown in Figs.(2), (3) are for explanatory purposes only)

Approximation in four unequal steps $\{0, \alpha, \beta, \alpha+\beta\}$ means to find α and β such that

$RMSDphase \approx \min$ according to Eq. (2). Level 1 takes zero value if $n < \alpha$, level 2 is α if $\alpha \leq n < \beta$, level 3 is β if $\beta \leq n < \alpha+\beta$,

and level 4 is $\alpha+\beta$ if $\alpha+\beta \leq n < 255$. The result is also a four-levels approximating phase map but with unequal steps $\Phi_{\Delta,U}$ (Fig. 3).

This kind of approximation adapts the partition of the interval $[0, 255]$ to the particular histogram subjected to

analysis. Moreover, since level 1 remains nailed down to zero it preserves the biasing to lower levels thus reducing the processing time.

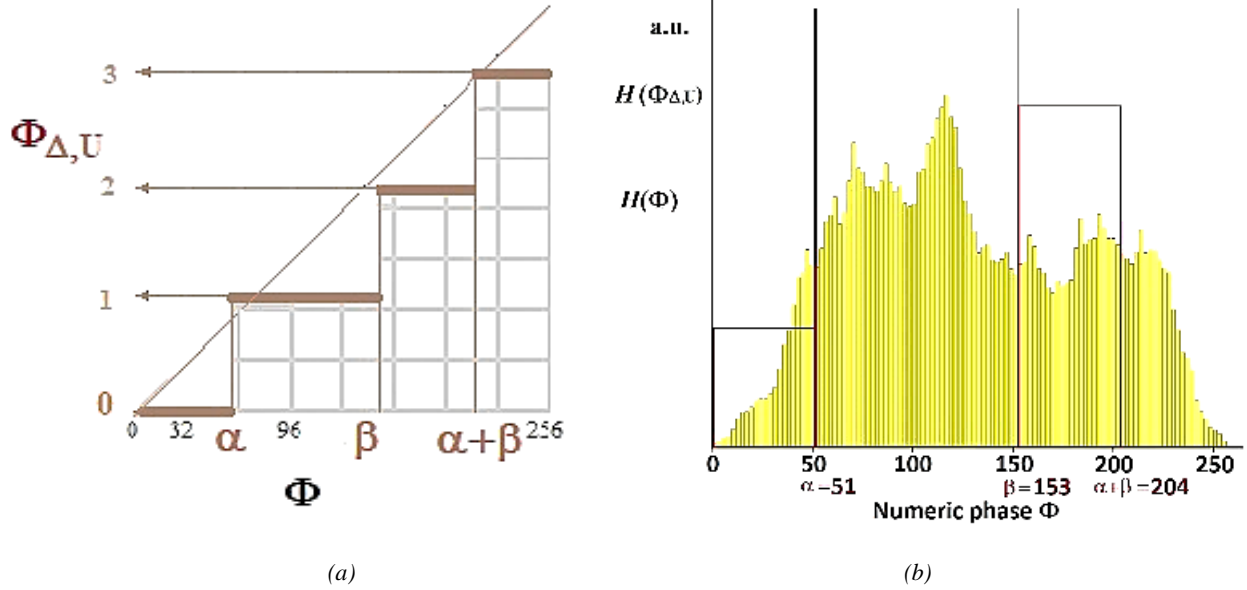


Fig. 3. (a) Approximation with unequal steps: the principle, and (b) the example of application on the same arbitrary histogram as in Fig. 2

The algorithm is implemented using the capabilities of Python software [12] where Eq. (2) is implemented in the equivalent form:

$$RMSD_{phase} = \sqrt{\frac{\sum_0^\alpha H(n) \cdot (n-0)^2 + \sum_{\alpha+1}^\beta H(n) \cdot (n-\alpha)^2 + \sum_{\beta+1}^{\alpha+\beta} H(n) \cdot (n-\beta)^2 + \sum_{\alpha+\beta+1}^{255} H(n) \cdot (n-\alpha-\beta)^2}{\sum_0^{255} H(n)}}. \quad (3)$$

In Fig. 4 are shown the approximations with four equal and unequal steps of a holographic phase map with 256 levels (the phase shifts were converted into gray levels).



Fig. 4. (a) Holographic phase map with 256 levels, (b) its approximations with four equal steps, and (c) with four unequal steps

2.3. Local optimization loop

Differing from the classical procedures where the approximation with equal phase steps is uniformly rounding the phase map $\Phi_{\Delta,E}(u,v) \approx \Phi_\delta(u,v)$ and consequently $O_{\Delta,E}(u,v) \approx O_\delta(u,v)$, here is introduced an additional, local optimization loop using the approximation with unequally phase steps $\Phi_{\Delta,U}(u,v) \approx \Phi_\delta(u,v)$, the indices E and U addressing the versions with equal and respectively unequal steps, see Fig. 5.

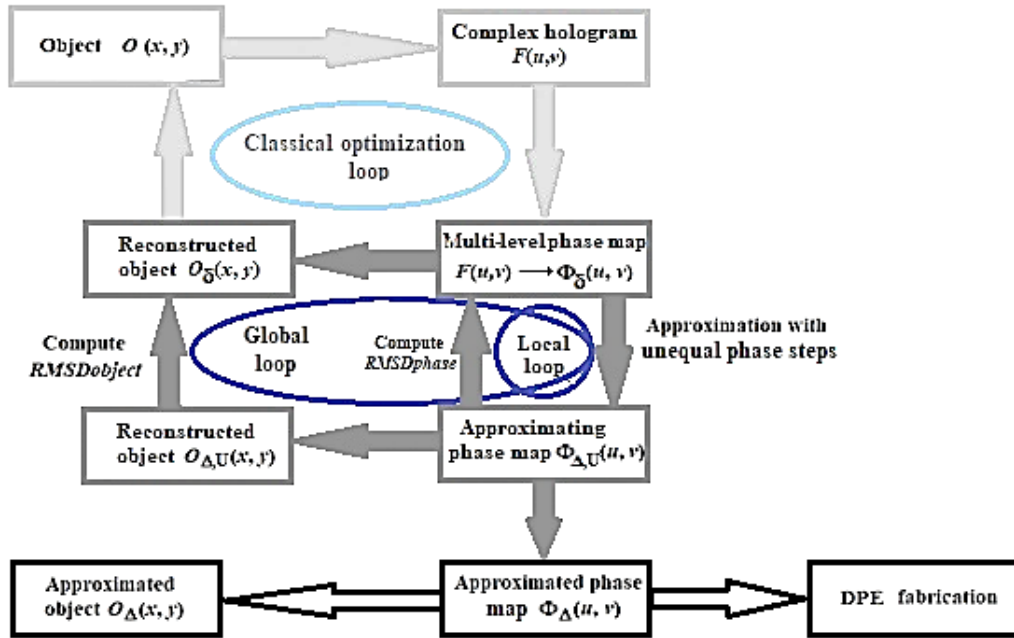


Fig. 5. Local optimization loop based on $RMSD_{phase}$ criterion and global loop based on $RMSD_{object}$ criterion

The additional approximation is supported by the assumption that despite the four steps truncation is worsening the 256-levels optimum, the process still remain inside the convergence area and the approximated object can still approach the desired object as the phase map is tracking the optimum phase map by unequal steps:

$$\Phi_{\Delta,U}(u, v) \rightarrow \Phi_{\delta}(u, v) \stackrel{S}{\Rightarrow} O_{\Delta}(x, y) \rightarrow O_{\delta}(x, y). \quad (4)$$

$$\begin{aligned} \sqrt{\frac{1}{IJ} \sum_{u,v} |\Phi_{\Delta,U}(u, v) - \Phi_{\delta}(u, v)|^2} &< \sqrt{\frac{1}{IJ} \sum_{u,v} |\Phi_{\Delta,E}(u, v) - \Phi_{\delta}(u, v)|^2} \stackrel{S}{\Rightarrow} \\ \stackrel{S}{\Rightarrow} \sqrt{\frac{1}{MN} \sum_{x,y} |O_{\Delta,U}(x, y) - O_{\delta}(x, y)|^2} &< \sqrt{\frac{1}{MN} \sum_{x,y} |O_{\Delta,E}(x, y) - O_{\delta}(x, y)|^2} \end{aligned} \quad (5)$$

The assumption stated by Eqs.(4), (5) has to be verified on the final results.

3. Results

3.1. Simulated phase distributions

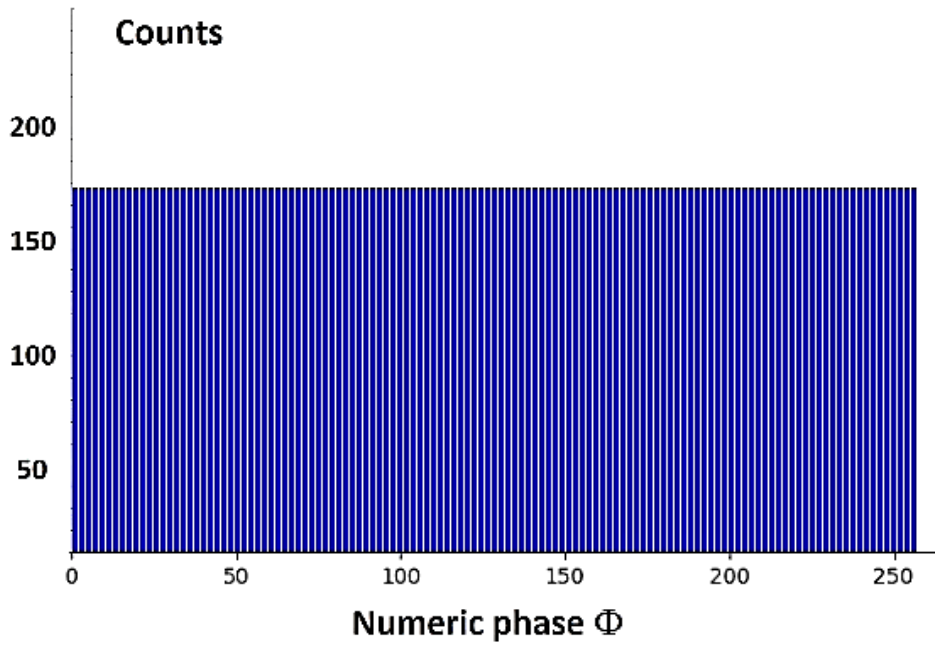
The way of how the unequal steps approximation adapts to several test histograms with 42000 elements each

In Eq.(4) the symbol $\stackrel{S}{\Rightarrow}$ means „resulting statistically” not uniformly.

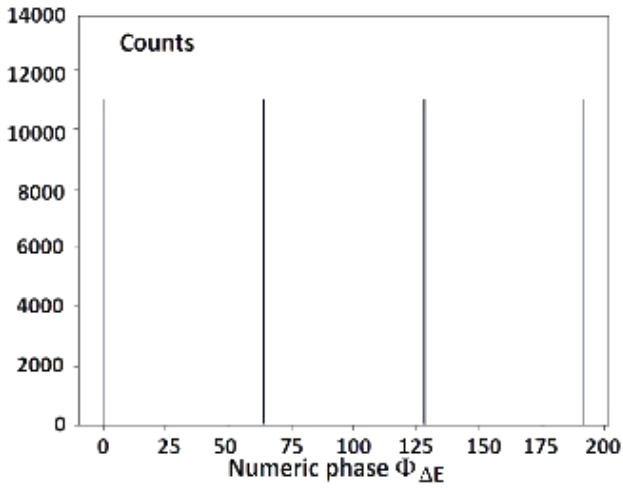
Although the relationship between convergences in object space and phase space remain a complex problem in the field of iterative algorithms [13], the additional iterative local loop based on unequal approximation can still minimize the $RMSDs$. More specifically:

is analyzed below. The representatives are histograms with uniformly distributed phase levels (type I), dominant low phase levels (type II), dominant high levels (type III), and dominant middle levels (type IV).

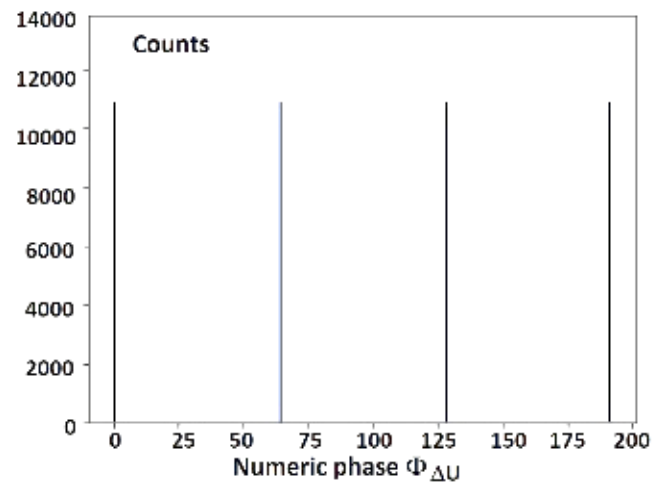
For type I (Fig. 6) the equal and unequal approximations coincide, i.e. the local loop outputs $\alpha=64$, $\beta=128$ and the method is not effective.



(a)



(b)

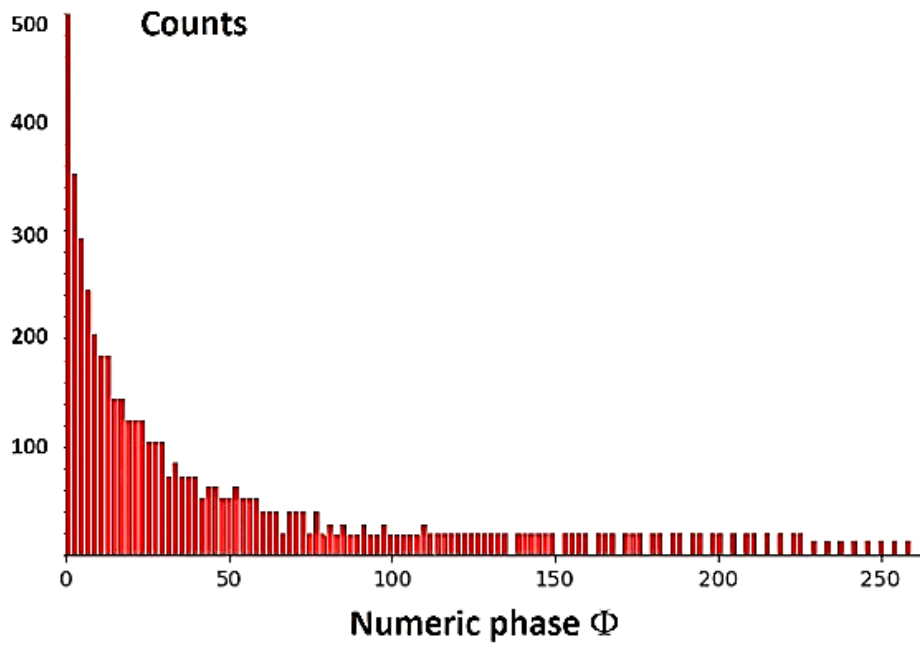


(c)

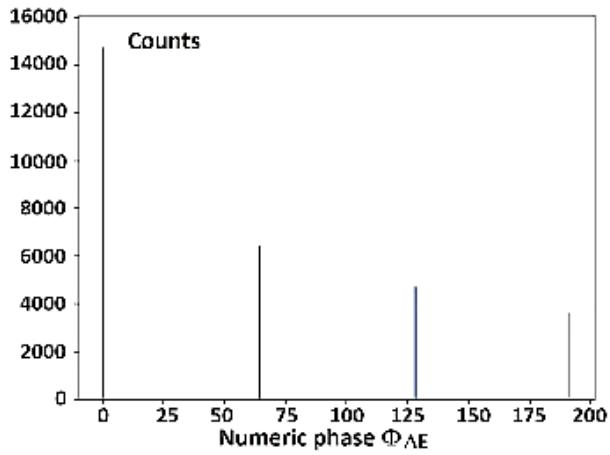
Fig. 6. (a) Uniformly distributed phase shifts: the associated histogram $H(\Phi)$, (b) the approximated version with four equal steps $H(\Phi_{\Delta E})$, and (c) the approximated version with four unequal steps $H(\Phi_{\Delta U})$ where $\alpha=64$, $\beta=128$

Type II and type III may result from nonlinear transforms, e.g. exponential or logarithmic that change the phase distribution across the polymer surface toward values which can eventually reduce the material consumption or the processing time. For example, to increase the area covered by the pixels with low phase shifts, one can apply an exponential law $\Phi_o(u, v) = a(e^{\frac{\Phi_i(u, v)}{b}} - 1)$, where $\Phi_o(u, v)$ is the value of the phase level attributed to the

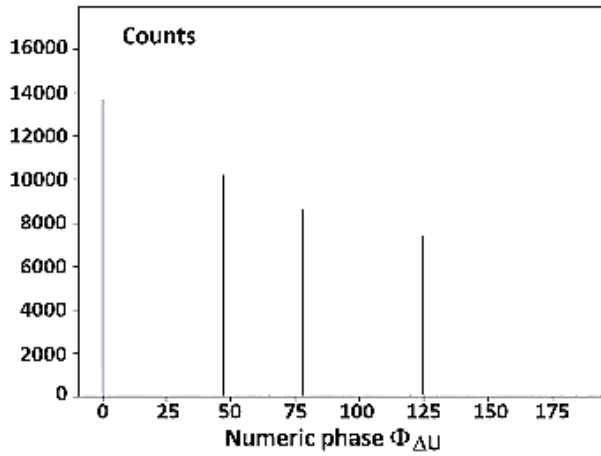
pixel of coordinates (u, v) in the output matrix, $\Phi_i(u, v)$ is the value of the phase level attributed to the pixel of coordinates (u, v) in the input matrix, a and b are regulatory parameters such that the interval $[0, 2\pi)$ be mapped onto itself [1]. The histogram shifts accordingly toward lower levels (Fig. 7).



(a)



(b)

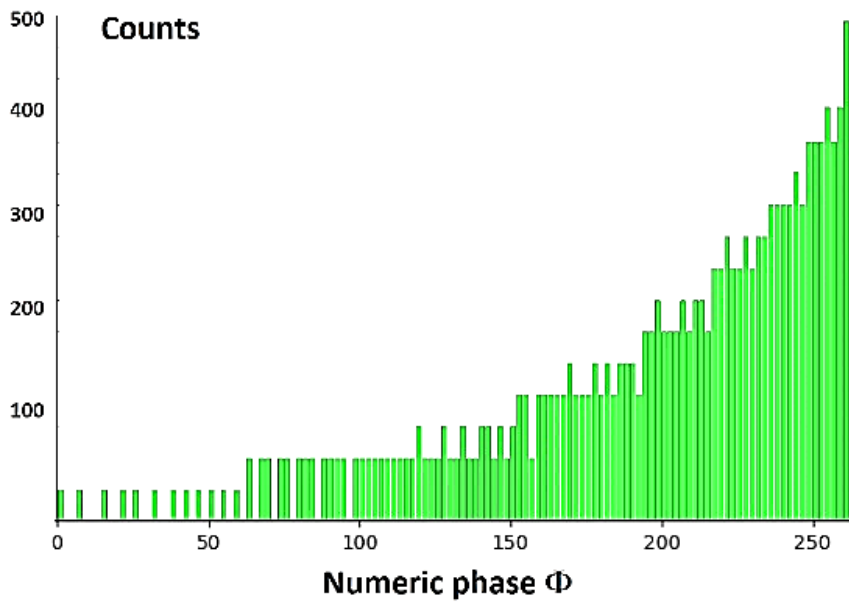


(c)

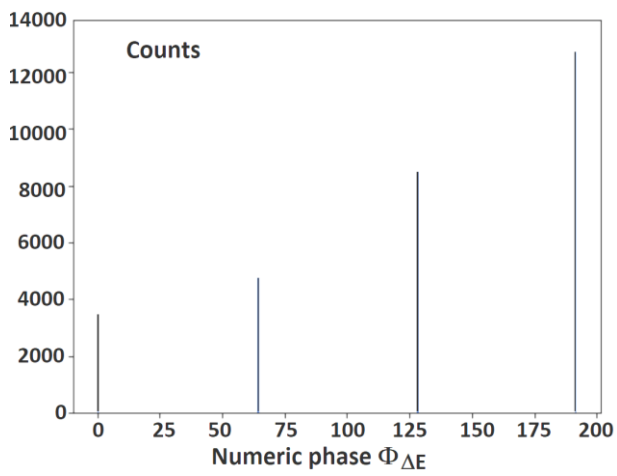
Fig. 7. (a) Dominant low phase shifts: the histogram $H(\Phi)$, (b) the approximated version with equal steps $H(\Phi_{\Delta E})$, and (c) the approximated version with unequal steps $H(\Phi_{\Delta U})$ where $\alpha=48$, $\beta=77$

Conversely, when applying a logarithm of the form $\Phi_o(u, v) = c \log(d\Phi_i(u, v) + 1)$ where c and d are fitting

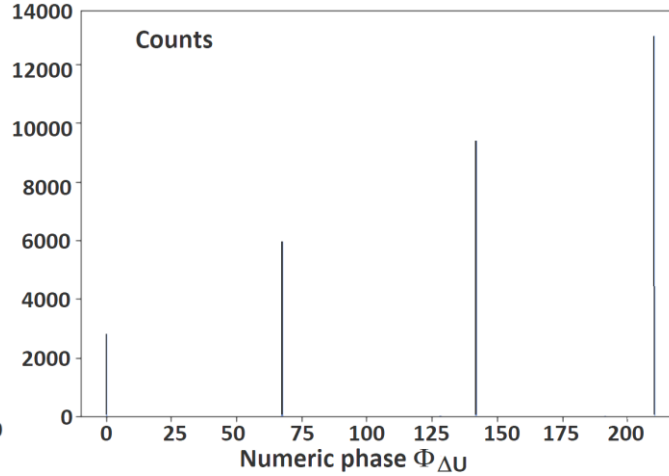
constants, the higher phase shifts are enhanced and the histogram shifts to the right (Fig. 8).



(a)



(b)



(c)

Fig. 8. (a) Dominant high phase shifts: the histogram $H(\Phi)$, (b) the approximated version with equal steps $H(\Phi_{\Delta E})$ (b), and (c) the approximated version with unequal steps $H(\Phi_{\Delta U})$ where $\alpha=69$, $\beta=142$

The combination of the previous rules gives a version with enhanced middle levels as shown in Fig. 9.

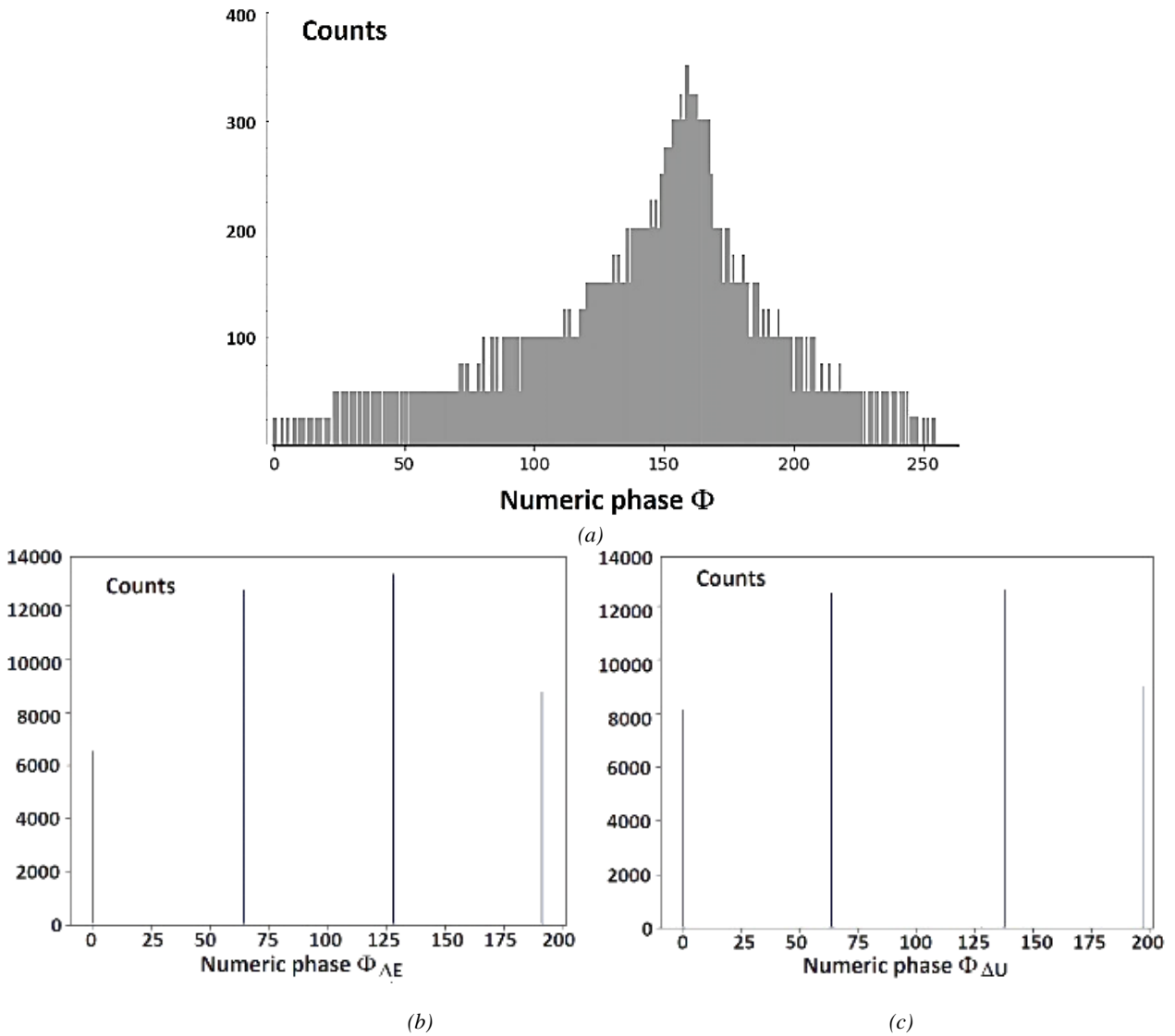


Fig. 9. (a) Dominant middle phase shifts: the histogram $H(\Phi)$, (b) the approximated version with equal steps $H(\Phi_{\Delta,E})$, and (c) the approximated version with unequal steps $H(\Phi_{\Delta,U})$ where $\alpha=62$, $\beta=137$

At least for single-peaked histograms considered here, one should remark the approximation with unequal steps has two visible effects upon $H(\Phi_{\Delta,U})$ as compared to $H(\Phi_{\Delta,E})$: i/ the dragging α and β toward the peak of the histogram $H(\Phi_{\delta})$, and ii/ the reducing the differences among the counts.

3.2. Validation on real holographic phase maps

The method was experimentally run on three holographic phase maps whose objects are sets of vortices denoted Object 1, Object 2, and Object 3 (Fig.10).

The holograms are designed by simulating the interference between tilted plane waves and helical Laguerre-Gauss modes [14, 15].

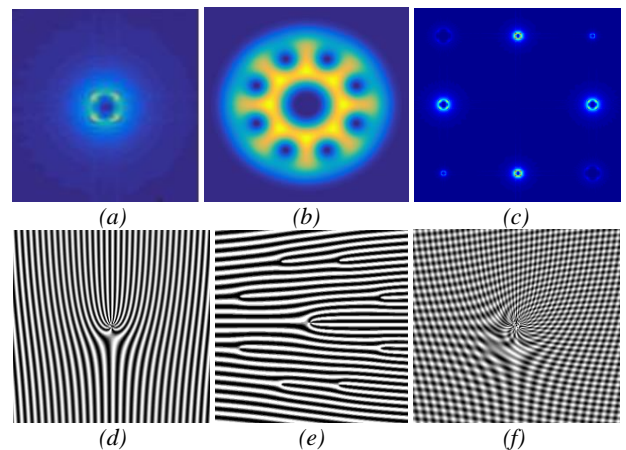


Fig. 10. (a) Object 1, (b) Object 2, (c) Object 3, and (d), (e), (f) their corresponding 256-levels holograms Φ_{δ}

The algorithm was run along the local loop for all three holograms by minimizing $RMSD_{phase}$ with respect to the reference 256-levels phase map Φ_s . They are computed in normalized units according to Eq. (3). In Fig. 11 are given the results of the approximations with four equal steps (shadowed zone), and with four unequal steps (no shadow) as well as the corresponding values of α and β in each case.

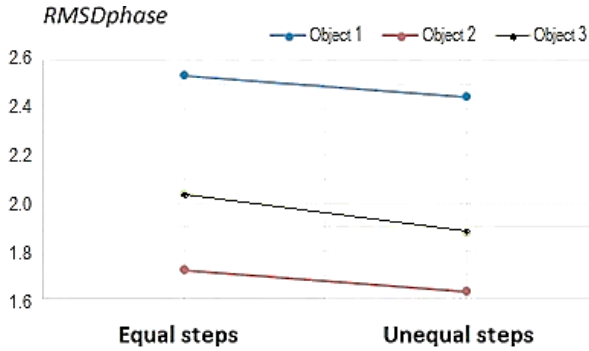


Fig. 11. $RMSD_{phase}$ in the cases of Object 1 ($\alpha=70$, $\beta=143$), Object 2 ($\alpha=65$, $\beta=120$), and Object 3 ($\alpha=69$, $\beta=137$)

To verify Eqs. (4), (5), for each object was computed $RMSD_{object}$ along the global loop with respect to the reference object O_s . All reconstructed objects were considered in the active area of the first diffracted order. The results are given in Fig. 12.

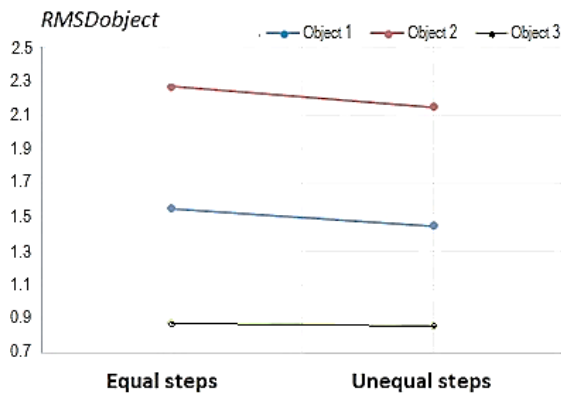


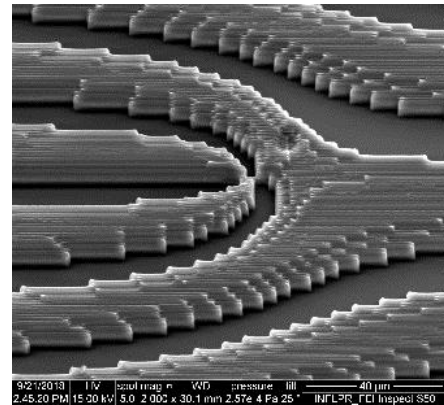
Fig. 12. $RMSD_{object}$ in the cases of Object 1, Object 2, and Object 3

In spite of the very small improvement in the case of Object 3, the approximations with unequal steps is reducing $RMSD_{object}$ in all investigated cases, therefore the assumptions stated by Eqs. (4) and (5) are valid and the algorithm remains inside the convergence radius.

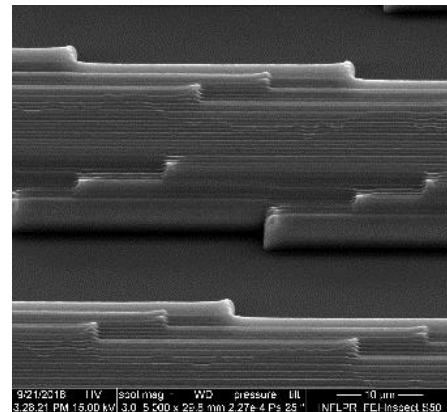
3.3. DPE fabrication by DLW-2PP

DPEs of millimeter sizes (1200×1200 pixels, $2 \mu\text{m}/\text{pixel}$) were subsequently fabricated with DLW-2PP technology (Photonic Professional Nanoscribe GMBH

[16]). We followed the standard typical processing methodology consisting in substrate cleaning, drop-casting of the photo-polymerizable material IPL-780 on glass substrate, laser irradiation, and sample development. As substrates we used $170 \mu\text{m}$ thick glass slides (BK7) cleaned with isopropanol. The photo-polymerizable materials were irradiated with 80MHz, 120fs laser pulses at $\lambda=780\text{nm}$ central wavelength. The positions of both laser focus and sample are controlled (the sample on XY-axes, the beam focus on Z-axis). For higher resolution processing we used three synchronized piezoelectric stages. The heights of DPEs are in micrometer range allowing for steps of hundreds of nanometers (4nm vertical position precision). After laser writing the DPEs require no other processing stages except the immersion in PGMEA developer solution for 3 minutes to wash away the non-polymerized material.



(a)



(b)

Fig. 13. (a) SEM images for DLW-2PP DPE approximated with four unequal steps, and (b) detail

The geometric heights of steps were computed after the value of the refractive index has been determined using scattering Scanning Near-Field Optical Microscopy measurements as described in [17, 18]. In the case of the polymer IPL-780 used here the value of the refractive index was 1.523 ± 0.002 at working wavelength of 632.8nm . SEM

images of the approximated DPE in four unequal steps corresponding to Object 2 are presented in Fig. 13.

The details are comparable to those reported in [19]. The diffracted beams after DLW-2PP DPEs with four unequal steps are shown in Fig. 14.

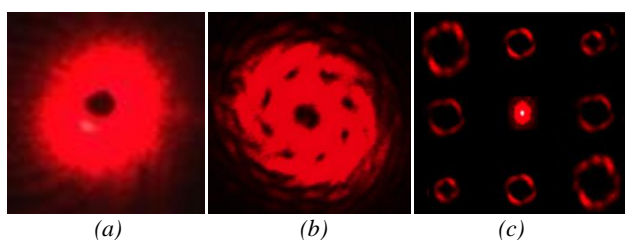


Fig. 14. Diffracted beams through DPEs with four unequal steps: (a) Object 1, (b) Object 2, and (c) Object 3

In the case of Object 2 the manufacturing time for DPE with 4 equal steps was 24 hours while for the DPE with 4 unequal steps it came down to 16 hours. The functional performances of the corresponding diffracted images were evaluated in terms of contrast

$$C = \frac{I_{\max} - I_{\min}}{I_{\max} + I_{\min}}, \quad (6)$$

where maximum and minimum intensities I_{\max} and I_{\min} were measured in the first diffraction order. In the case of DPE with 4 unequal steps the contrast was $88.82 \pm 1.51\%$ compared to $85.36 \pm 1.23\%$ in the case of DPE with 4 equal steps.

4. Conclusions

A method to optimize the design of the diffractive phase elements based on unequal steps approximation with consequences on reducing the fabrication time and on slightly improving the optical performances of the diffracted images is presented. For the same number of digitized steps, the results are evidencing the advantages of approximation with unequal steps versus the equal ones at least in the cases we have chosen here. A local iterative loop based on evaluation of the root mean square distance in the phase plane statistically improves the characteristics of the reconstructed object in terms of intensity distribution. The method is less effective in the case of holograms exhibiting phase shifts close to uniformly shaped distributions. The method is an acceptable compromise between preserving relevant micro-relief details and accurate image reconstruction under the constraint of limited number of imprinting steps. Practical application of the method is facilitated by the versatility of direct laser writing with two-photon polymerization technology.

Acknowledgements

Research supported by Romanian Ministry for Scientific Research and Innovation UEFISCDI, PN-III-P2-2.1-PED-2016-1396, #218PED/2017.

References

- [1] V. A. Soifer, Computer Design of Diffractive Optics, Elsevier, 2012.
- [2] T.-L. Chang, S.-W. Luo, H. P. Yang, C. H. Lee, Microelectr. Eng. **87**(5-8), 1344 (2010).
- [3] M. Mihailescu, A. Craciun, R. A. Gabor, C. A. Nicolae, M. Pelteacu, B. Comanescu, G. Bostan, UPB. Sci. Bull. A **80**(2), 259 (2018).
- [4] K. Switkowski, A. Anuszkiewicz, A. Filipkowski, D. Pysz, R. Stepien, W. Krolikowski, R. Buczynski, Opt. Expr. **25**(24), 31443 (2017).
- [5] A. Trichili, C. Rosales-Guzmán, A. Dudley, B. Ndagano, A. Ben Salem, M. Zghal, A. Forbes, Sci. Rep. **10**(6), 27674 (2016).
- [6] D. Preece, S. Keen, E. Botvinick, R. Bowman, M. Padgett, J. Leach, Optics Express **16**(20), 15897 (2008).
- [7] X.-F. Li, S.O'Brien, R.J. Winfield, J. Optoelectron. Adv. M. **12**(3), 595 (2010).
- [8] R. W. Gerchberg, W. O. Saxton, Optik **35**, 237 (1972).
- [9] L. Ionel, C. P. Cristescu, Optoelectron. Adv. Mat. **5**(9), 906 (2011).
- [10] M. Guillon, B.C. Forget, A.J. Foust, V. De Sars, M. Ritsch-Martel, V. Emiliani, Optics Express **25**(11), 12640 (2017).
- [11] O. Carugo, and S. Pongor, Protein Science: A Publication of the Protein Society **10** (7), 1470 (2001).
- [12] J. V. Guttag, (2016-08-12), Introduction to Computation and Programming Using Python: With Application to Understanding Data, MIT Press, 2016.
- [13] M. Norrlöf, S. Gunnarsson, Int. J. Control **75**(14), 1114 (2002).
- [14] R. Tudor, M. Mihailescu, I. A. Paun, A. E. Nan, M. Kusko, C. Kusko, Proc. of the Rom. Acad. Series A **17**, 222 (2016).
- [15] R. Tudor, M. Mihailescu, C. Kusko, I. A. Paun, A. Nan, M. Kusko, Opt. Comm. **368**, 141 (2016).
- [16] https://www.nanoscribe.de/en?pk_campaign=company_nanoscribe&pk_kwd=nanoscribe&gclid=EAIaIQobChMIhuvE_YeK3QIVCMayCh1XxQasEAAYASAAEgKMqPD_BwE.
- [17] D. E. Tranca, S. G. Stanciu, R. Hristu, C. Stoichita, S. A. M. Tofail, G.A. Stanciu, Sci. Rep-UK **5**, 11876 (2015).
- [18] D. E. Tranca, S. G. Stanciu, R. Hristu, B. M. Witgen, G. A. Stanciu, Nanomed-Nanotechnol. **14**(1), 47 (2018).
- [19] A. Jurkevičiūtė, N. Armakavičius, D. Virganičius, L. Šimatonis, T. Tamulevičius, S. Tamulevičius, J. Optoelectron. Adv. M. **19**(3), 119 (2017).

*Corresponding author: eugen_scarlat@yahoo.co.uk